Multi-view 3D CG Image Quality Evaluation and Analysis for Application Procedure between H.265/HEVC and Watermarking

Norifumi Kawabata
Center for Frontier Medical Engineering,
Chiba University
1-33 Yayoi-cho, Inage-ku, Chiba, Japan
norifumi@chiba-u.jp; norifumi@nagoya-u.jp

***Abstract*—In our previous studies, we studied on the multi-view 3D CG image quality evaluation including visible digital watermarking. Particularly, we verified for the multimedia evaluation including both the coded image quality and watermark quality. Actually, the image quality of watermarking is not always better in case we carried out the visible digital watermarking. Therefore, depending on the situation, we need to change the coded image quality of watermarking. In this paper, we used 3D CG images with 8 viewpoints parallax barrier method, which embedded the watermarking image encoded and decoded by H.265/HEVC in advance by transforming frequency domain for the generated images. And then, we composed the generated images. We carried out the subjective quality evaluation of these images, and then we analyzed results, and classified evaluation values by using Support Vector Machine (SVM). Furthermore, we considered for the application procedure of watermarking by comparing mutually to the case of considering the coded image quality of watermarking.**

Keywords—Multi-view 3D Image; Coded Image Quality; Watermark Quality; Wavelet Transformation; Double Stimulus Impairment Scale (DSIS); Support Vector Machine (SVM)

I. INTRODUCTION

It is advanced for the preparation towards beginning of general broadcasting for Quad FHDTV (QFHDTV, 4K) image quality four times more than Full HDTV (FHDTV). By improvement of image quality, 3D image and video are focused as one of added values. On the other hand, from 2015 to 2016, VR (Virtual Reality) boom comes in Japan. VR, AR (Augmented Reality), and MR (Mixed Reality) are based on 3D image and video technology. As the related work, at present, it is advanced for the research and development of multi-view 3D image and video processing and quality assessment. For use of still image and video, it is important for assessment focused on their contents. At present, from users' view, they are able to add and embed various information since we are able to watch video by mobile or smartphone, video on-demand service. Therefore, it is problem for copyright or security, and it is an important theme for contents assessment on information hiding performance and digital watermarking. In previous studies on visible digital watermarking for images, there were many cases of using frequency domain transformation. For the coded quality, there were many studies on image watermark methods using JPEG coding, H.264/AVC. For stereoscopic images, there were the proposed method based on wavelet transformation with binocular method [1], the assessments on Depth Image Based Rendering (DIBR) 3D [2], [3]. For medical image engineering field, there were approaches using 3D images and watermark as shown in [4].

To the present, we were studying for 8 viewpoints 3D CG image quality assessment including visible digital watermarking. In the case of embedding watermark for images, we processed watermarking by frequency domain transformation for encoded and decoded images by H.265/HEVC. However, in fact, watermarking image quality is not always good in the case of the processing for visible digital watermarking. Therefore, depending on situation, we consider that we need to change the watermarking image quality.

In this paper, we processed embedding by using frequency domain transformation for watermarking image encoded and decoded by H.265/HEVC in advance, and then, we carried out the subjective evaluation experiment for generated images with 8 viewpoints parallax barrier method. Next, we analyzed for experiment results, and we classified subjective evaluation values for Quantization Parameter (QP), embedding intensity (Q) by using Support Vector Machine (SVM). On the other hand, we discussed for application procedure of visible digital watermark by comparing to the case of no considering watermark quality.

II. IMAGE QUALITY EVALUATION

A. 3D CG Images and Watermarking Images in This Study

In this study, we used 3D CG image contents "Museum (M)," "Wonder World (W)" provided by NICT [5] for no charge as shown in Fig. 1 (a)-(d). For watermarking images, we used evaluation images "Port view (Pv)," "Flower pot (Fp)" provided by IHC [6] for no charge as shown in Fig. 1 (e)-(f). For the generation of multi-view images, as shown in Fig. 2 and 3, first, we constructed 8 viewpoints cameras on Computer Graphics (CG), and carried out the processing of camera work, rendering [7]. And then, we generated still images by 8 viewpoints. Next, we processed dividing two types of (1), (2) as follows.

(1) We processed of watermark for 3D CG images by 8 viewpoints encoded and decoded by H.265/HEVC [8].

978-1-5386-2615-3/18/$31.00 ©2018 IEEE

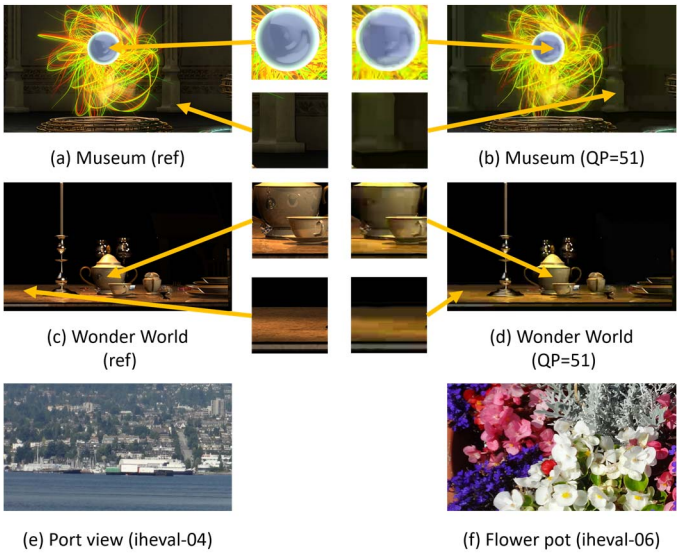

Fig. 1: 3D CG images and watermarking images used in this study

(2) We processed of watermark for watermarking images (IHC images) encoded and decoded by H.265/HEVC.

Finally, we generated 3D CG images by 8 viewpoints, and obtained evaluation images.

In this study, we carried out two types of experiments as follows.

(1) In the case of no considering the coded image quality for watermark (Experiment 1: Exp. 1)

(2) In the case of considering the coded image quality for watermark (Experiment 2: Exp. 2)

For image sequences, we prepared 144 types of image sequences including types of Quantization Parameter (QP) ((1) $QP = 0, 20, 30, 40, 51$ (2) $QP = 0, 20, 25, 30, 35, 40, 51$), types of CG contents. For detail of watermark processing, we will explain the next subsection II B. For watermark arrangement by frequency domain, we set two level of three level, since the arrangement of two level is middle level of three level and then we will able to estimate evaluation value of one level and three level.

B. Embedding Method for Image Watermarking in This Study

For embedding of watermarking image, we processed using wavelet transformation. We show the generation procedure in the following.

[1]. Decompose the original and watermarking images into R, G, and B components.

Perform DWT (Discrete Wavelet Transformation) for the R, G, and B component images generated by RGB decomposition. For this study, we performed wavelet transformation using the filter bank 5/3 tap SSKF (Simple Short Kernel Filter). Figure shows the ten-bandwidth sub-band region obtained by three-level octave division. In general, the LL signal is the low frequency component for the horizontal and vertical directions, and shows an approximate image of the image signal in order to focus the image signal energy on the low component. On the other hand, sub-band LH, HL, and HH signals show the horizontal, vertical, and diagonal direction components, respectively.

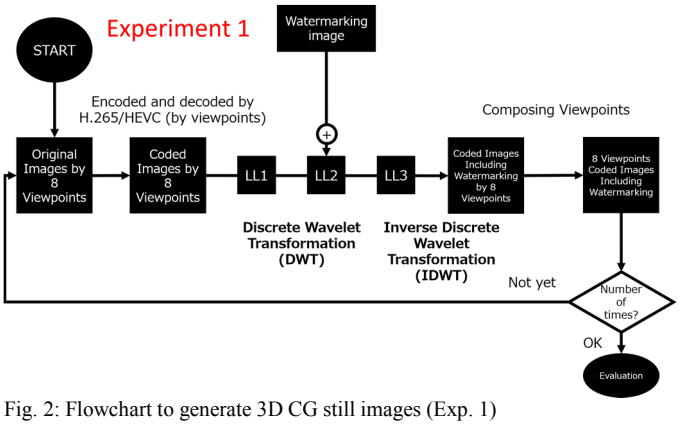

Fig. 2: Flowchart to generate 3D CG still images (Exp. 1)

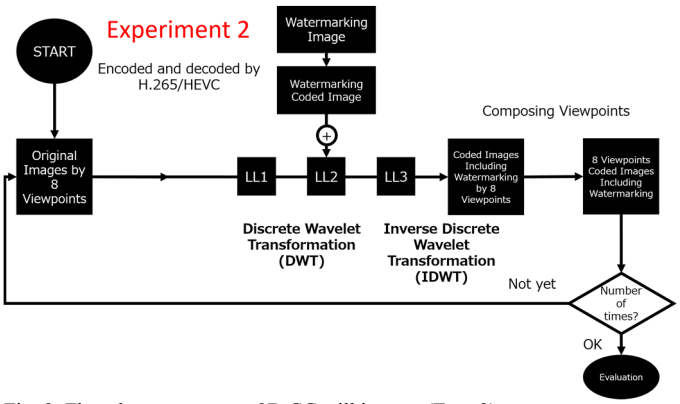

Fig. 3: Flowchart to generate 3D CG still images (Exp. 2)

TABLE I: Main specification of subjective quality assessment

Type of display	Newsight 3D Display 24V type	
Display resolution	1920×1080 (Full HD) (pixel)	
Display resolution in the case of presentation	1920×960 (pixel)	
Types of 3D CG images	"Museum" (M), "WonderWorld" (W)	
Types of image	Windows bitmap	
Encoding and decoding	H.265/HEVC	
Quantization Parameter (QP)	(1) QP=0 (ref), 20, 30, 40, 51 (2) QP=0 (ref), 20, 25, 30, 35, 40, 51	
Types of digital watermarking images	"Port view" (iheval-04, Pv), "Flower pot" (iheval-06, Fp) digital watermarking by wavelet transformation	
Frequency domain component	"LL2"	
Embedding intensity (Q)	Q=0.01, 0.05, 0.1	
3D system	Parallax Barrier Method	
The number of viewpoints	Only 8 viewpoints	
Visual range	3H (Height of an image)	
Indoor lighting	None (same as dark room)	
Assessor's position	Within horizontally ±30° from the center of the screen	
Evaluation experiment	Presentation time	10 seconds/Contents
	Evaluation method	Double Stimulus Impairment Scale
	Assessor	Repeating 5 times by an assessor

[2]. For an image by sub-band division, we designated each the difference region for R, G, and B components. Then, embed the watermarking onto the sub-band image by a linear combination of the image. After the watermarking process, sub-band image I_w is obtained as indicated in Eq. (1).

$$I_w = \sum_{i=1}^{M} \sum_{j=1}^{N} \{A_{ij} + \alpha_{ij} B_{ij}\} \qquad (1)$$

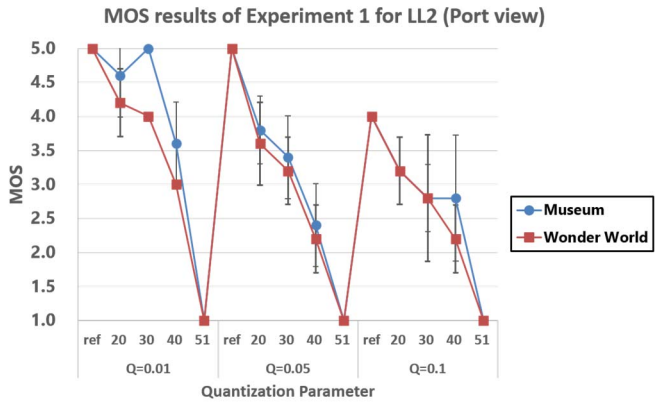

Fig. 4: MOS results of Exp. 1 (Port view)

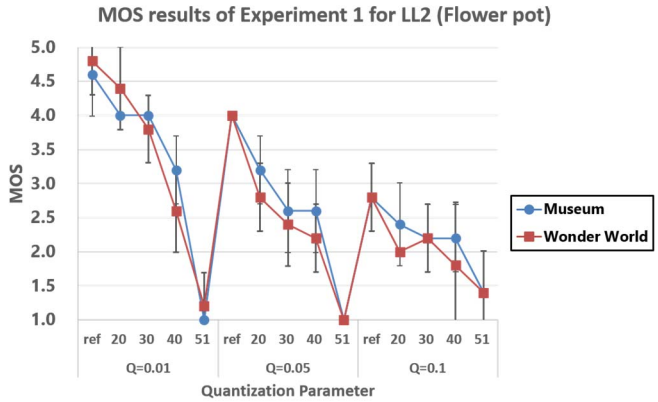

Fig. 5: MOS results of Exp. 1 (Flower pot)

Here, M is the horizontal direction of the image signal, N is the vertical direction of the image signal, A is the coded image, B is the watermarking image, and α is the weight coefficient, that is, embedding intensity Q of the watermarking image. After completing the processing, for each sub-band region, we set up α as flat and the weight coefficient of A as one.

[3]. Compose the watermarking resulting image of the R, G, and B components obtained by IDWT (Inverse Discrete Wavelet Transformation). Finally, the generated image is obtained.

C. *Experimental Contents*

TABLE I shows specification of experiments in this study. Experimental environment is based on ITU-R BT.500-13 Recommendation [9], and we carry out experiments in dark room. For 3D display, we used multi-view parallax barrier display in this study. In the pixel arrangement, each viewpoint is arranged consistently as R, G, and B in the direction of the right diagonal. In the 3D display mechanism, the images can be seen in the 3D display from different fields of view by dividing R, G, and B through the parallax barrier in front of an LCD display. When we displayed a 3D image on the 3D display, we performed real-time parallax mix automatically using a media player provided by Newsight Corporation [10]. Furthermore, we defined the CG camera interval based on the experiment results [11].

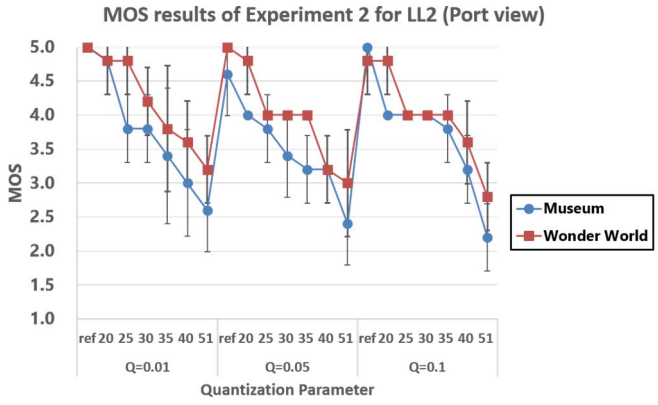

Fig. 6: MOS results of Exp. 2 (Port view)

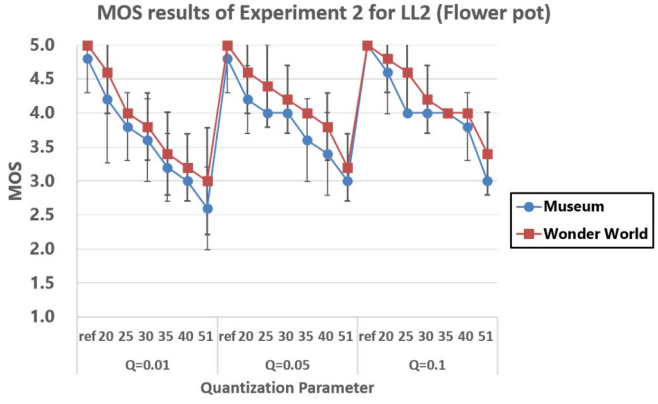

Fig. 7: MOS results of Exp. 2 (Flower pot)

D. *Experimental Method and Evaluation Method*

For experimental method, we carried out experiments based on DSIS (Double Stimulus Impairment Scale). First, we displayed reference image A for 10 seconds, and then mid-gray image G for 3 seconds. Next, we displayed test condition image B for 10 seconds. Subsequently, the assessor evaluated this cycle and inputted the assessment value into the computer application (VOTE), which required 10 seconds. This cycle was defined as one set, and we repeated the cycle until the last set. It is as practical environment for us to analyze a lot of data speedy by outputting CSV (Comma-Separated Values) files.

For evaluation method, we used EBU (European Broadcasting Union). The assessors assigned evaluation scores according to five ranks (MOS: Mean Opinion Score (M_{MOS}, W_{MOS})). Here, we defined $MOS = 4.5, 3.5, 2.5$ as "DL (Detective Limit)," "AL (Acceptability Limit)," and "EL (Endurance Limit)," respectively. For this study, each assessor repeated the evaluation five times [12].

III. Experimental Result and Discussion

A. *Experimental Results*

Figs. 4 and 5 show MOS ("Pv," "Fp") results of Exp. 1. Figs. 6 and 7 show MOS ("Pv," "Fp") results of Exp. 2. The vertical line of Figs. 4–7 is MOS (M_{MOS}, W_{MOS}). The horizontal line of Figs. 4–7 is the Quantization Parameter (QP). The error bar is

TABLE II: Correctly classified percentage of SVM (Exp. 1)

Class	Total Number of Instances	Correctly Classified Instances	Percentage	Mean absolute error	Root mean squared error
QP ("Pv")	75	54	72%	0.26	0.34
Q ("Pv")	75	44	58.7%	0.33	0.43
QP ("Fp")	75	44	58.7%	0.27	0.36
Q ("Fp")	75	48	64%	0.33	0.43

TABLE III: Correctly classified percentage of SVM (Exp. 2)

Class	Total Number of Instances	Correctly Classified Instances	Percentage	Mean absolute error	Root mean squared error
QP ("Pv")	105	55	52.4%	0.22	0.32
Q ("Pv")	105	42	40%	0.40	0.50
QP ("Fp")	105	44	41.9%	0.22	0.33
Q ("Fp")	105	49	46.7%	0.39	0.49

extended vertically from the plot points in Figs. 4–7, which shows 95% confidence interval.

From results of Exp. 1, for "Pv", the difference among QP is large. On the other hand, for "Fp", the higher Q is, the smaller the difference among QP is. Particularly, in the case of Q=0.05, for QP=ref, 20, the difference of M_{MOS} and W_{MOS} is between 0.5 and 1. From this, in case Q is low, the influence of the coded degradation is higher than that of embedding intensity, on the other hand, in case Q is high, the influence of embedding intensity is higher than that of the coded degradation. Therefore, we considered that it is easy for assessors to perceive affect.

From results of Exp. 2, overall, $W_{MOS} > M_{MOS}$ is satisfied. Therefore, MOS in 40 of 42 patterns are more than "EL". In the case of the coded image quality of watermark, we consider that there is affection of the coded image quality or contents than the embedding intensity. From result of Exp. 2, we obtained as knowledge that MOS is between "AL" and "DL" at least.

From experimental data of subjective quality evaluation, we classified evaluation values for some classes by using SVM (Support Vector Machine) by SMO (Sequential Minimal Optimization) algorithm. From TABLE II, III, overall, correctly classified percentage of Exp. 2 is lower than that of Exp. 1. Therefore, we judged as "classified" in Exp. 1, and judged as "not classified" in Exp. 2.

B. Discussion

From experimental results, the evaluation score (Mean Opinion Score (MOS)) on processing of coding for watermarking image is higher than that on processing of coding for watermarked image, however, QP change rate on processing of coding for watermarking image is lower than that on processing of coding for watermarking image. We consider that it is not easy to perceive if the coded degradation is occurred. In terms of watermarking, if some information is embedded for watermarking images, it is enabled to hide information more than adding that for watermarked image. If it is not interfered for assessors to evaluate, the evaluation condition is good. However, if there were embedding information for images, it is not easy to perceive for watermarked image, and evaluation score is better in the subjective evaluation. We can judge this from results of assessment classification by SVM. Overall, from experimental results, we need to carry out the objective evaluation for parts of no judgement by subjective evaluation, and we need to consider generation evaluation in addition to subjective evaluation.

IV. CONCLUSION

From results of this study, the case of coding for watermarking image is higher evaluation scores than that for watermarked image. However, as a whole of contents evaluation, it is not easy for assessors to perceive information addition. Therefore, we consider that this is the relation between trade-off.

As future works, from experimental results, we consider that the coded image quality, luminance, lightness of contents, background than the embedding intensity are affected. Therefore, we will see as target of assessment for the other image characteristics or medical imaging. A part of this study is supported by Prof. Masaru Miyao, and supported by research grant for Ph.D. student from Nagoya University. Thanks.

REFERENCES

[1]. Y. Chen and H. Huang, "A Wavelet-based Image Watermarking Scheme for Stereoscopic Video Frames," *2013 Ninth International Conference on Intelligent Information Hiding and Multimedia Signal Processing*, pp.25--28, 2013.

[2]. H. Kim, J. Lee, T. Oh, and H. Lee, "Robust DT-CWT Watermarking for DIBR 3D Images," *IEEE Transactions on Broadcasting*, Vol.58, No.4, pp.533--543, Dec. 2012.

[3]. L. Chen and J. Zhao, "Watermarking Based Quality Assessment for DIBR 3D Images," *2016 IEEE International Conference on iThings and IEEE GreenCom and IEEE CPSCom and IEEE Smart Data*, pp.810--814, 2016.

[4]. H. Mohaghegh, N. Karimi, S. M. R. Soroushmehr, S. Samavi, and K. Najarian, "Adaptive stereo medical image watermarking using non-corresponding blocks," *2015 37th Annual International Conference on EMBC*, Aug. 2015.

[5]. NICT, http://www.nict.go.jp/, accessed Nov. 10, 2017.

[6]. IHC evaluation image, http://www.ieice.org/iss/emm/ihc/image/image.php, accessed Nov. 10, 2017.

[7]. Autodesk, http://www.autodesk.co.jp/, accessed Nov. 10, 2017.

[8]. F. Bossen, D. Flynn, K. Sühring, "HM Software Manual," https://hevc.hhi.fraunhofer.de/svn/svn_HEVCSoftware/, accessed Nov. 10, 2017.

[9]. ITU-R BT.500-13, http://www.itu.int/rec/R-REC-BT.500, accessed Nov. 10, 2017.

[10]. Newsight, http://newsightjapan.jp/, accessed Nov. 10, 2017.

[11]. N. Kawabata and Y. Horita, "Statistical Analysis of Subjective Assessment for 3D CG Images with 8 Viewpoints Lenticular Lens Method," *IIEEJ Trans. on Image Electronics and Visual Computing*,Vol.4, No.2, pp.101--113, Dec. 2016.

[12]. N. Kawabata and M. Miyao, "3D CG Image Quality Metrics by Regions with 8 Viewpoints Parallax Barrier Method," *IEICE Trans. on Fundamentals*, Vol.E98-A, No.08, pp.1696--1708, Aug. 2015.